Experimental Study Online Detection of Toluene Secondary Organic Aerosol by Synchrotron Radiation Vacuum Ultraviolet Photoionization Mass Spectrometer

Mincong Zhu [1], Mingqiang Huang [1,*], Xiaobin Shan [2], Liusi Sheng [2], Xingqiang Liu [3], Weixiong Zhao [4], Xuejun Gu [4], Weijun Zhang [4*]

[1] Fujian Provincial Key Laboratory of Modern Analytical Science and Separation Technology, College of Chemistry & Chemical Engineering and Environment, Minnan Normal University, Zhangzhou 363000, China.

[2] National Synchrotron Radiation Laboratory, University of Science and Technology of China, Hefei 230031, China.

[3] School of Environment Science & Engineering, Tan Kah Kee College, Xiamen University, Zhangzhou 363105, China.

[4] Laboratory of Atmospheric Physico-Chemistry, Anhui Institute of Optics and Fine Mechanics, Chinese Academy of Sciences, Hefei 230031, China.

Supplementary Information

To whom correspondence should be addressed
*Email : huangmingqiang@mnnu.edu.cn, wjzhang@aiofm.ac.cn

Content

S1 Calibration information for SMPS and GC-FID

For each experiment, the scanning mobility particle sizer (SMPS) and gas chromatography with flame ionization detector (GC-FID) were calibrated as follows before use. The SMPS system (3080L DMA, 3775 CPC, TSI Corporation, USA, stable SNR above 100) was strictly calibrated following standard aerosol measurement specifications before and during the experiment. Flow rate calibration was performed quarterly using a NIST-traceable flow standard to ensure the accuracy of sheath flow and sample flow with a relative error lower than ±1%. For particle size calibration, NIST-certified polystyrene latex (PSL) standard particles with diameters of 50 nm, 100 nm, and 200 nm were adopted to verify the mobility-diameter conversion relationship of the instrument. The counting efficiency of the condensation particle counter was calibrated annually against a standard reference aerosol electrometer. All raw particle size distribution data were automatically corrected for particle charging efficiency, instrumental diffusion loss, and counting deviation via the official supporting software, ensuring the reliability of aerosol measurement data.

The GC-FID system (7820A, Agilent Technologies, USA, signal-to-noise ratio (SNR) greater than 100) was calibrated in accordance with atmospheric detection standard methods. Gas path parameters including carrier gas, hydrogen and air flow rates were calibrated monthly with a high-precision digital flowmeter, and the temperature of the injection port, chromatographic column oven and FID detector was regularly verified to eliminate temperature deviation. A five-point external standard calibration curve was established using NIST-traceable VOC mixed standard gas covering all experimental concentration ranges, with the linear correlation coefficient $R^2 \geq 0.999$. Daily calibration verification was conducted with medium-concentration standard samples, and the relative standard deviation (RSD) of peak area repeatability was controlled within 2%. The limit of detection (LOD) and limit of quantification (LOQ) were determined based on the signal-to-noise ratio of 3 and 10, respectively, guaranteeing the accuracy and reproducibility of gas-phase component qualitative and quantitative analysis.

S2 Mass spectra for toluene fine particles at photon energy of 10.5 eV under different temperature of heated plate

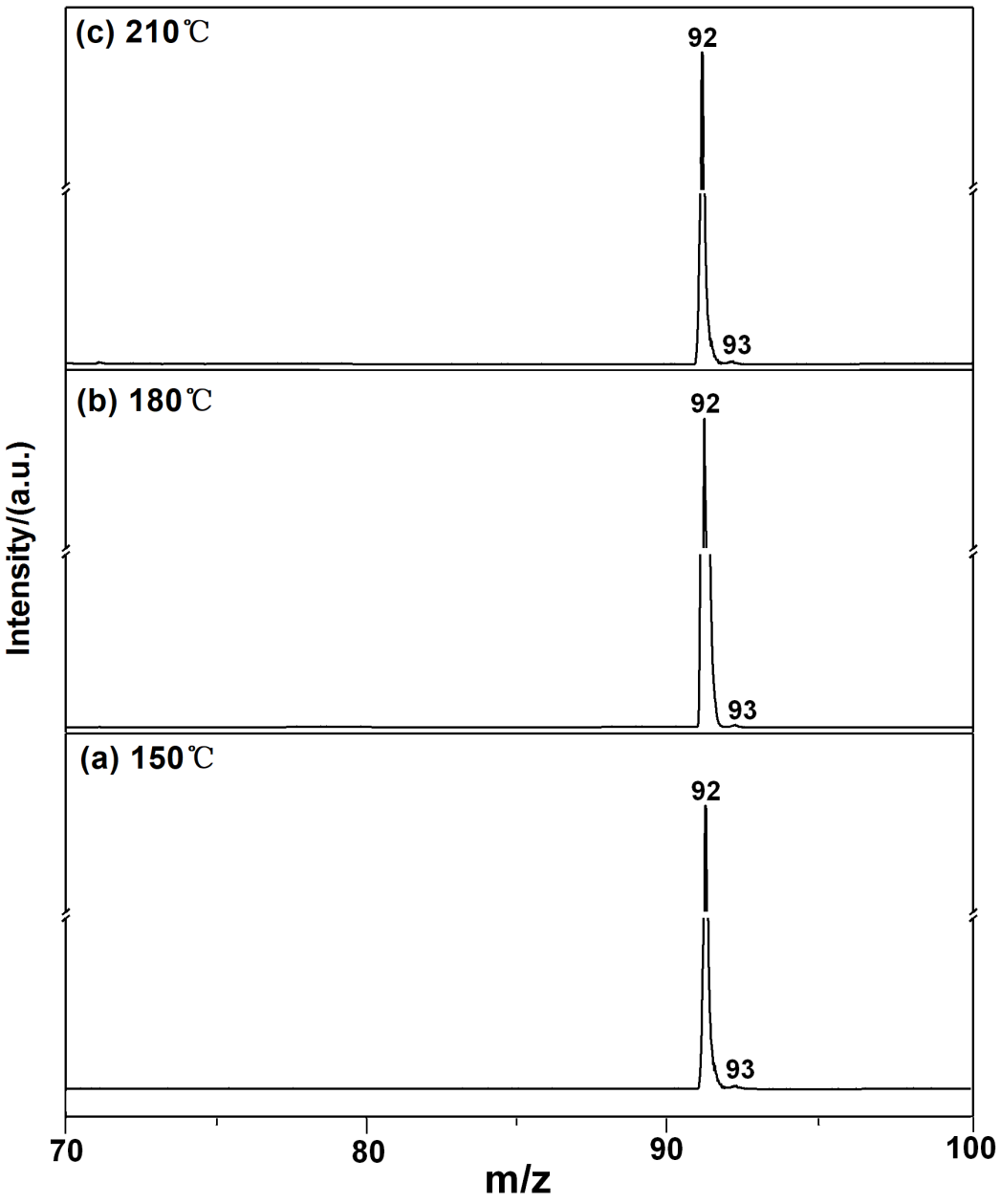

Fig.S1. Mass spectra for toluene fine particles at photon energy of 10.5 eV under the temperature of heated plate was set to (a) 150℃, (b)180℃ and (c) 210℃.

S3 Explanation of how wall-loss correction

Wall loss is formed when aerosol particles deposit on the wall of smog chamber due to turbulence, Brownian diffusion and gravitational sedimentation. The wall loss depends on the particle size and can be described as a first order process dependent on particle loss coefficient, $k_{dep}(d_p)$:

$$\frac{dN(d_p)}{dt} = -k_{dep}(d_p)N(d_p) \quad (1)$$

where $N(d_p)$ is the number concentration of particles and $k_{dep}(d_p)$ is the loss coefficient for particles with diameter d_p [1-3]. To determine the loss rate of aerosol particles, based on our previous experiments [4-6], four independent experiments are conducted under dark conditions. $(NH_4)_2SO_4$ particles are generated using TSI 9302 (TSI Corporation, USA), and the number concentration of particles for different sizes at different times is measured by scanning mobility particle size analyzer (SMPS, 3080L DMA, 3775 CPC, TSI Corporation, USA) to obtain their attenuation rate. To avoid the condensation between aerosol particles, the initial aerosol number concentration is less than 10^3 cm^{-3}. **Fig. S1** shows the relationship between the experimentally measured aerosol wall loss coefficient $k_{dep}(d_p)$ and aerosol particle size d_p. According to the experimental results of Takekawa et al. (2003), $k_{dep}(d_p)$ has the following relationship with d_p:

$$k_{dep}(d_p) = ad_p^b + c / d_p^d \quad (2)$$

The experimental data are subjected to nonlinear least squares fitting using Equation (2), and the parameters a, b, c, and d are obtained as 4.17×10^{-13}, 4.66, 10.18, and 0.75, respectively. For aerosol particles with d_p of 300 nm, k_{dep} is calculated to be 28.7%·h^{-1}, which is larger than that reported by Takekawa et al. (2003) (10.3 % h^{-1}). This is mainly because the volume of chamber used in this study (850 L) is smaller than that of Takekawa et al. (2003) (2000 L).

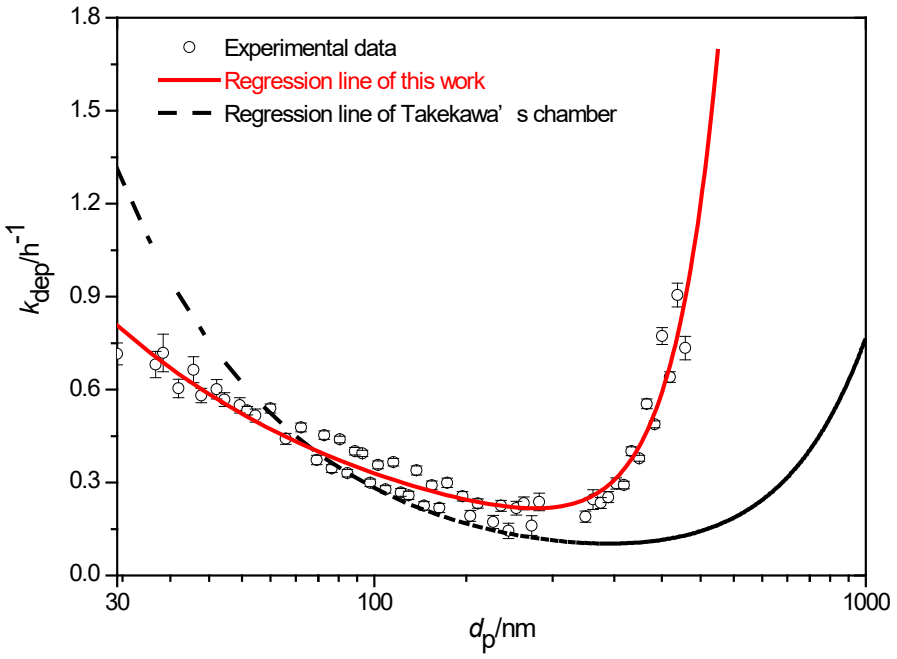

Fig. S2. The deposition rate efficient (k_{dep}) of the particles as the function of particle diameter(d_p)

Reference

1. COCKER D.R., MADER B.T., KALBERER M., FLAGAN R.C., SEINFELD J.H. The effect of water on gas-particle partitioning of secondary organic aerosol: II. m-xylene and 1,3,5-trimethylbenzene photooxidation systems. Atmospheric Environment, **35** (35), 6073, **2001.**
2. HUANG M.Q., HAO L.Q., CAI S.Y., GU X.J., ZHANG W.X., HU C.J., WANG Z.Y., FANG L., ZHANG W.J. Effects of inorganic seed aerosols on the particulate products of aged 1,3,5-trimethylbenzene secondary organic aerosol. Atmospheric Environment, **152**, 490, **2017.**
3. TAKEKAWA H., MINOURA H., YAMAZAK S. Temperature dependence of secondary organic aerosol formation by photo-oxidation of hydrocarbons. Atmospheric Environment 37 (24), 3413, 2003.
4. XU J., HUANG M.Q., CAI S.Y., LIU X.Q., HU C,J., GU X,J., FANG L., ZHANG W.J. Mass spectral analysis of the aged 1,3,5-trimethylbenzene secondary

organic aerosol in the presence of ammonium sulfate seeds. Polish Journal of Environmental Studies, **26** (4), 1531, **2017**.

5. WANG W.C., HUANG M.Q., HU H.M., ZHAO W.X., HU C.J., GU X.J., ZHANG W.J. Characterization of chemical components and optical properties of toluene secondary organic aerosol in presence of ferric chloride fine particles. Atmosphere, **14** (7), 1075, **2023**.
6. HUANG M.Q., SHAN X.B., SHENG L.S., WANG Z.Y., HU C.J., GU X.J., ZHANG W.J. On-line measurement of styrene secondary organic aerosol using synchrotron radiation vacuum ultraviolet photoionization aerosol mass spectrometer. Chinese Journal of Analytical Chemistry, **52** (8), 1200, **2024**.

S4 Mass spectra of toluene SOA measured by Aerodyne aerosol mass spectrometer

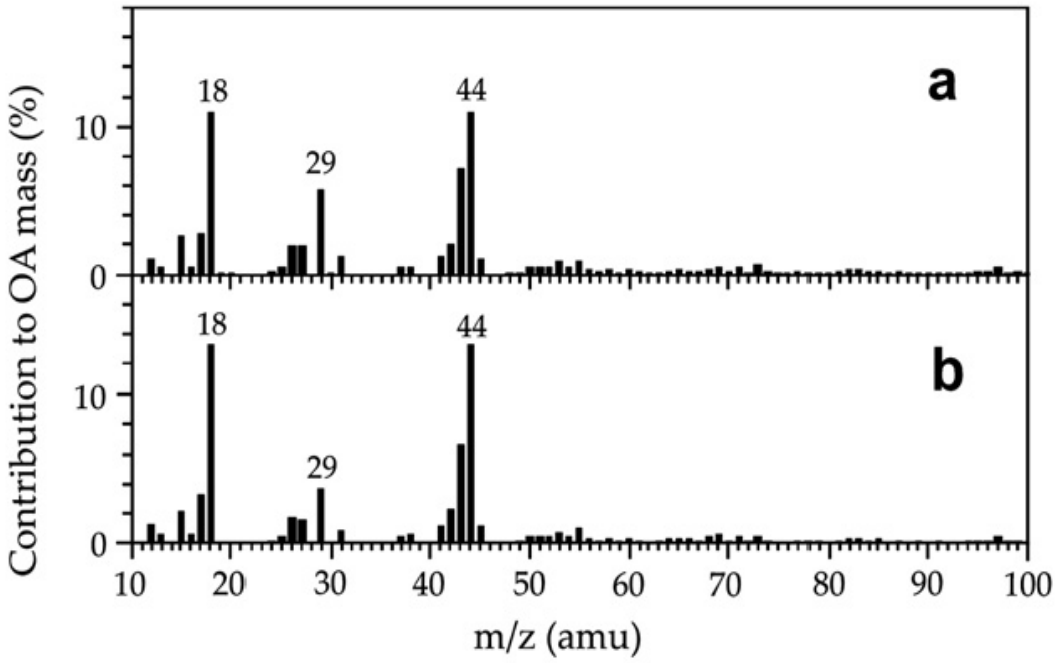

Fig. S3. Organic aerosol mass spectra measured at (a) 2.1 h and (b) 11.4 h after the start of irradiation in an experiment with toluene reported by Sato et al. [1].

Reference

1. SATO K., TAKAMI A., ISOZAKI T., HIKIDA T., SHIMONO A., IMAMURA T. Mass spectrometric study of secondary organic aerosol formed from the photo-oxidation of aromatic hydrocarbons. Atmospheric Environment, **44** (8), 1080, **2010.**